Solid State Communications 250 (2017) 119–122

Contents lists available at ScienceDirect

Solid State Communications

journal homepage: www.elsevier.com/locate/ssc

Communication

e-beam irradiation effects on IR absorption bands in single-walled carbon nanotubes

Masao Ichida[a,*], Katsunori Nagao[a], Yuka Ikemoto[b], Toshiya Okazaki[c], Yasumitsu Miyata[d], Akira Kawakami[e], Hiromichi Kataura[c], Ikurou Umezu[a], Hiroaki Ando[a]

[a] Department of Physics, Konan University, 8-9-1 Okamoto, Higashinada-ku, Kobe 658-8501, Japan
[b] Japan Synchrotoron Radiation Research Institute and SPring-8, 1-1-1 Kouto, Sayo-cho, Sayo-gun, Hyogo 679-5198, Japan
[c] Nanotube Research Center, Advanced Industrial Science and Technology, Central 4, 1-1-1 Higashi, Tsukuba, Ibaraki 305-8562, Japan
[d] Department of Physics, Faculty of Science, Tokyo Metropolitan University, 1-1 Minami-Ohsawa, Hachioji, Tokyo 192-0397, Japan
[e] National Institute for Information and Communications Technology, 588-2 Iwaoka, Nishi-ku, Kobe 651-2492, Japan

ARTICLE INFO

Keywords:
A. Single-walled carbon nanotubes
D. Plasmon resonance
E. IR absorption spectra

ABSTRACT

We have measured the absorption and Raman spectral change induced by the irradiation of e-beam. By the irradiation of e-beam on SWNTs thin films, the intensity of defect related Raman band increase, and the peak energy of IR absorption bands shift to the higher energy side. These results indicate that the origin of infrared band is due to the plasmon resonance of finite-length SWNT. We have estimated the effective tube length and defect density from IR absorption peak energy.

1. Introduction

Many considerable research efforts have been done to investigate the optical and dielectronic properties in single-walled carbon nanotubes (SWNTs) from the viewpoint of both basic research and device applications. For example, the linear and nonlinear optical properties in SWNTs have been studied in order to clarify the electronic states in 1 dimensional carbon systems and to evaluate SWNTs as new materials for optical devices [1]. In the absorption spectra for semiconducting and metallic SWNTs, the intrinsic absorption bands can be observed between near infrared to ultra-violet region, which are due to the optical transition between valence and conduction bands with exciton effects [2–5]. Although, there are no corresponding intrinsic electronic states, the broad absorption bands appear in infrared (IR) region for both semiconducting and metallic SWNTs [6–10]. The origins of these IR absorption bands have been discussed for more than ten years. Two models have been proposed for the origin of IR bands, which are mini-gap transition and plasmon resonance. The experimental results on the temperature dependence of the absorption spectra [6] and results of pump-probe measurement [8] in the far-infrared region suggest that the far-infrared absorption band is due to interband mini-gap transitions in the nanotubes. Simple theoretical studies also predict that only the “armchair” SWNT is truly metallic and that other “metallic” SWNTs have a small energy gap [11–13]. Other theoretical studies suggest that the bundled metallic SWNTs have a small pseudo energy gap [14]. On the other hand, tube length dependence of IR absorption spectra has been reported [7,10], which suggests that the origin is geometric plasmon resonance. In the previous paper, we have studied absorption spectra of high purity metailc and semiconducting SWNTs in wide energy region from 0.001 to 5 eV [9]. For both metallic and semiconducting SWNTs, IR absorption bands appear at around 0.02 – 0.2 eV. We have discussed the origin of IR absorption bands for both metallic and semiconducting SWNTs, but we could not determine. In this study, we have irradiated e-beam to the high purity semiconducting and metallic SWNTs thin film samples, and investigated the origin and irradiation effects on the IR absorption bands.

2. Samples and experimental

The high purity metallic and semiconducting SWNT thin films are prepared by using the density-gradient ultracentrifugation (DGU) method [15]. The surfactant and other contamination were carefully removed as described in the previous work. For optical measurements, purified SWNTs are placed on quartz or Si substrates. The thickness of the SWNT thin films is about 300 nm. In these thin film samples, SWNTs are bundled as confirmed by X-ray diffraction. The diameter of bundle is about 5 nm. The absorption spectra have been measured by using UV–VIS spectrometer and micro-FTIR spectrometer with synchrotron radiation at SPring-8 BL43IR beamline. The e-beam has been irradiated by using scanning electron microscope (JEOL JSM-6400)

* Corresponding author.
E-mail address: ichida@konan-u.ac.jp (M. Ichida).

http://dx.doi.org/10.1016/j.ssc.2016.11.023
Received 28 July 2016; Received in revised form 14 September 2016; Accepted 27 November 2016
Available online 28 November 2016

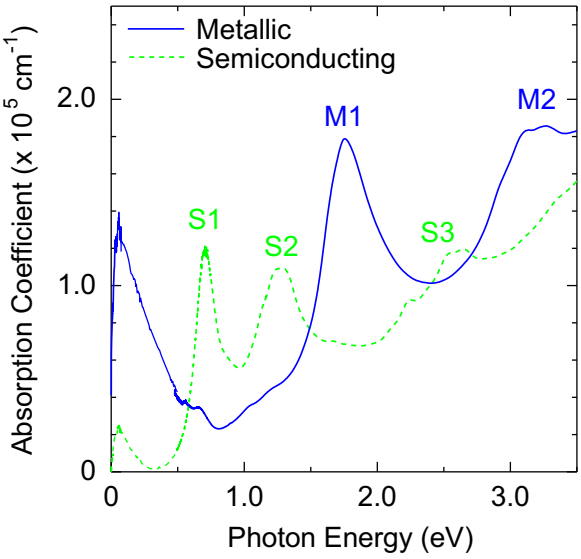

Fig. 1. (Color online) Absorption spectra of high purity semiconducting (broken curve), and metallic (solid curve) SWNT thin films.

with accelerating voltage of 15 kV. All spectra have been measured at room temperature.

The dotted curve in Fig. 1 shows the near-infrared and visible absorption spectra of semiconducting SWNT thin films. Broad absorption bands are observed at 0.70 eV (S1), 1.24 eV (S2), and 2.60 eV (S3). These bands correspond to the optical transition between valence and conduction bands with exciton effects. In the case of the high purity metallic SWNT sample (solid curve), both the M1 band and M2 bands can be observed at about 1.8 eV and 3.2 eV, which correspond to the first and second band to band transitions. From these absorption spectra of the high purity samples, we can estimate the mean tube diameter and purity of both the metallic and semiconducting SWNT samples. The estimated tube diameter is about 1.4 nm and purities are higher than 95%. As we have reported in the previous paper, broad absorption bands are observed below 0.5 eV for both semiconducting and metallic samples [9].

3. Results and discussion

Fig. 2(a) shows the Raman spectra of semiconducting SWNTs for pristine and e-beam irradiated samples. The G- and D-mode Raman peaks are observed at 1590 cm^{-1} and 1350 cm^{-1}, respectively. These spectra are normalized by the peak intensity of G-mode. The sample which shows the dotted curve spectrum is more strongly irradiated than dashed one. With increasing e-beam irradiation, the Raman intensity of D-mode increases, and the ratio of intrinsic G-mode to D-mode (G/D) decreases from 17.2 (pristine) to 10.4 (strongly irradiated). The D-band Raman peak is connected to defects in SWNT sp^2 bonds network. This result indicates that the defect density in SWNT increases with e-beam irradiation. Fig. 2(b) shows the absorption spectra in IR energy region for the same samples on a log-energy scale. By the e-beam irradiation, the S1 absorption band is decreased and broadened. This is consistent with the increase of defect density as seen in Raman spectra. At the same time, the IR absorption band shifts to the higher energy side with decreasing intensity. If this IR absorption band originated from the defect states in SWNT, the absorption intensity should increase by the e-beam irradiation. However, as seen in Fig. 2(b), the intensity of IR-band decreases. Thus, the defect states in SWNT are not appropriate to the origin of IR-band. Fig. 3(a) and (b) show the Raman and IR absorption spectra of metallic SWNTs for pristine and e-beam irradiated samples. In analogy with the case of semiconducting SWNTs seen in Fig. 2, the Raman intensity of D-mode

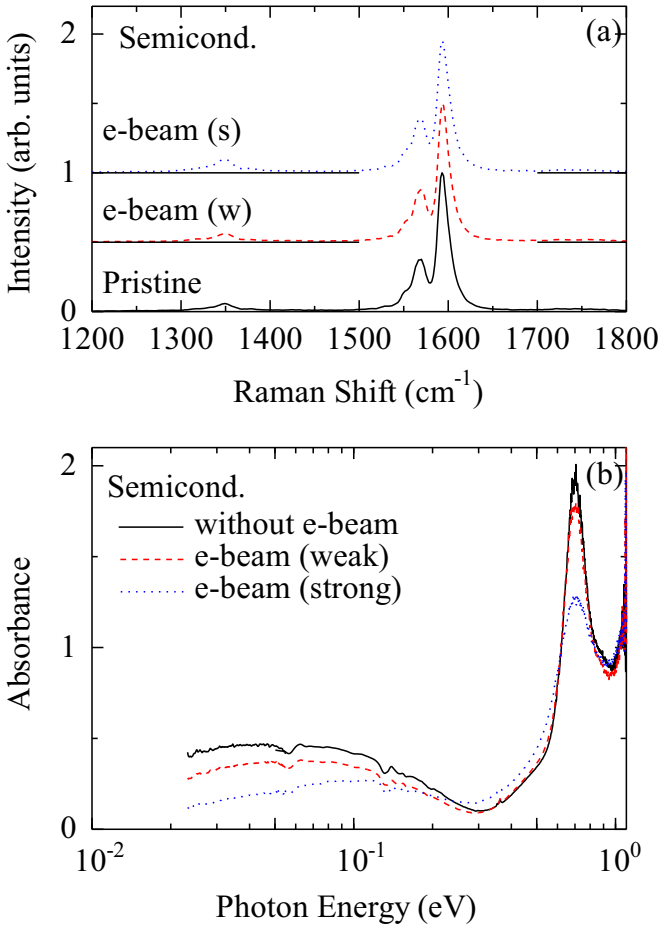

Fig. 2. (Color online) (a) Raman spectra of pristine and e-beam irradiated semiconducting SWNT samples. (b) Absorption spectra of the same samples in Raman spectra (a).

increases and IR absorption peak shifts to the higher energy side with increasing e-beam irradiation.

Recently, the IR absorption spectra have been calculated as a resonance of finite-length SWNT and electromagnetic wave [16]. According to this model, the resonant frequency f is proportional to the inverse of SWNT length L, such as,

$$f = \frac{v_p}{2L}, \tag{1}$$

where v_p is the Plasmon velocity in the SWNT. In fact, Morimoto et al. have reported that the peak energy position in IR absorption spectra for SWNTs linearly scaled with the inverse of tube length which has been measured by AFM [10]. They have also discussed the relation of the resonance energy to the defect density. In the real SWNTs, many defects exist and the distance between defects plays as an effective tube length L_{eff} for the resonance. Let us assume the number of defect in the SWNT as N_D, L_{eff} can be written as,

$$L_{eff} = \frac{L}{N_D + 1}, \tag{2}$$

and we should use this effective tube length instead of the real tube length for Eq. (1). The G/D ratio has often used to evaluate the quality of crystalline of SWNTs. If the intensity of D-mode is proportional to the defect density $n_D = N_d/L$, and the defect density is large, the effective tube length can be written as,

$$L_{eff} \approx \frac{L}{N_D} = \frac{1}{n_D} = a(G/D), \tag{3}$$

where (G/D) is the value of G/D ratio, and a is the constant. Thus, the resonant frequency is expressed as

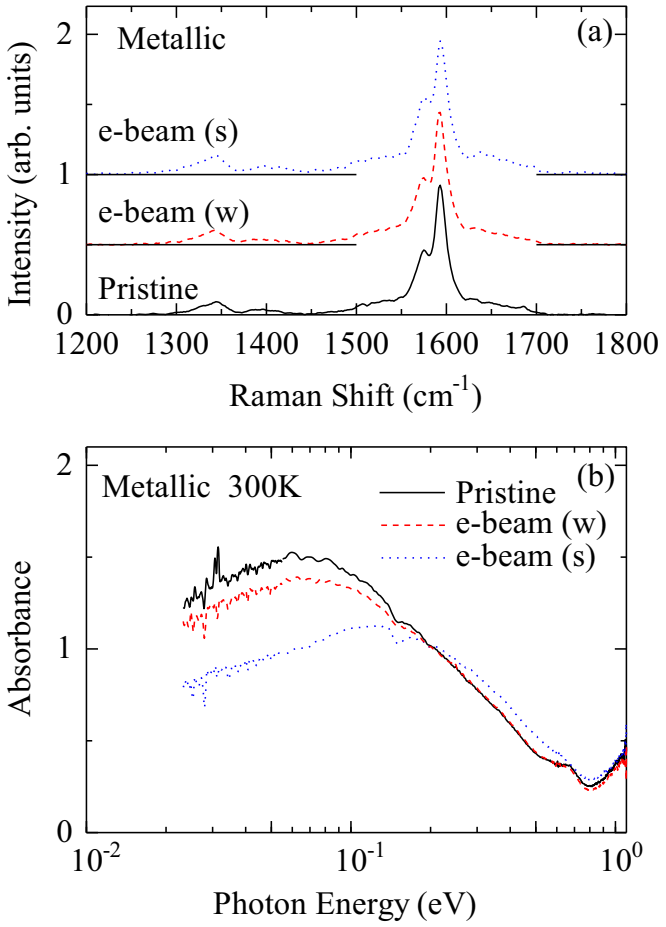

Fig. 3. (Color online) (a) Raman spectra of pristine and e-beam irradiated metallic SWNT samples. (b) Absorption spectra of the same samples in Raman spectra (a).

$$f = \frac{v_p}{2L_{eff}} = \frac{v_p}{2a(G/D)}. \quad (4)$$

Fig. 4(a) shows the relation of inverse of G/D ratio and the peak energy of IR absorption bands with different e-beam irradiated samples. If the IR absorption band originated from the mini-gap transition, the peak energy does not depend on the defect density. However, as seen in Fig. 4, the peak energy increases with decreasing the value of G/D ratio. It is approximately proportional to the inverse of G/D ratio. This experimental result indicates that the origin of IR absorption band for both metallic and semiconducting SWNTs are due to the plasmon resonance with the effective tube length. If we assume the plasmon velocity is 3.2×10^6 m/s [10], we can estimate the effective tube length and defect density. Fig. 4(b) shows the estimated effective tube length as a function of G/D ratio calculated by Eq. (4). The effective tube length linearly increase from 0.05 μm with G/D value of 7.1–0.14 μm with G/D value of 15.6. Because the average tube length is about 1 μm [17], the estimated effective tube length may be reasonable. The defect density also can be estimated by using Eqs. (3) and (4). In Fig. 4(a), the estimated defect densities are shown as the right side axis. Using this model, we can evaluate the defect density from G/D ratio.

It is worth while to mention the origin of IR absorption band in high purity semiconducting SWNTs sample. In our previous paper, we have suggested that the origin of IR band was related to the defect states [9]. However, as seen in Fig. 3, the absorption intensity of IR band decreases with increasing defect density. Thus, it is difficult to consider defect states as the origin of IR band. Fig. 5 shows IR absorption spectra for pristine and annealed semiconducting SWNTs thin film. By annealing the sample at 500 K in vacuum, the intensity of IR absorption band decreases. It is well known that the electronic

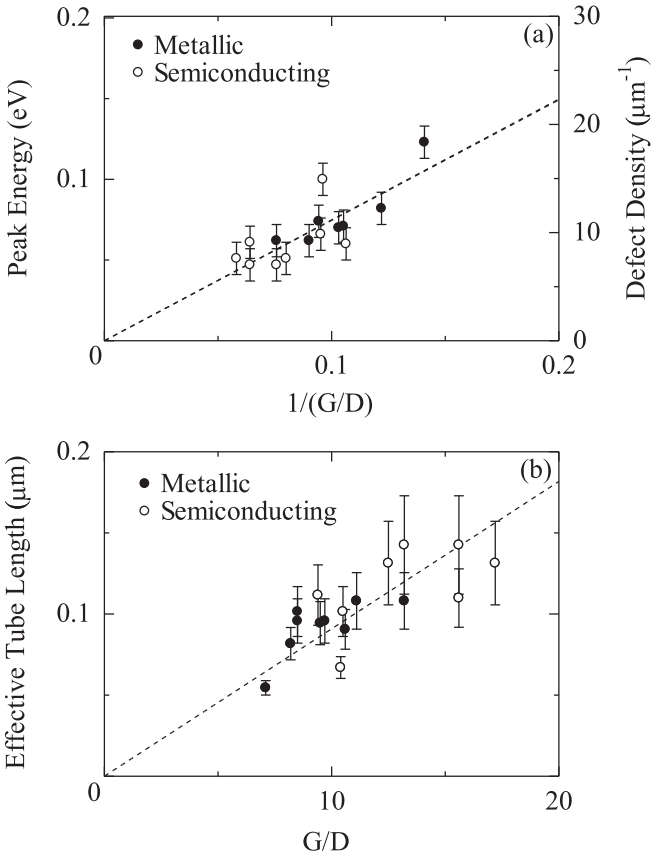

Fig. 4. (Color online) (a) The relation of inverse of G/D ratio and peak energy of IR absorption band (left axis) for both semiconducting and metallic. Estimated defect density is shown by right axis. (b) Estimated effective tube lengths are shown as a function of G/D ratio.

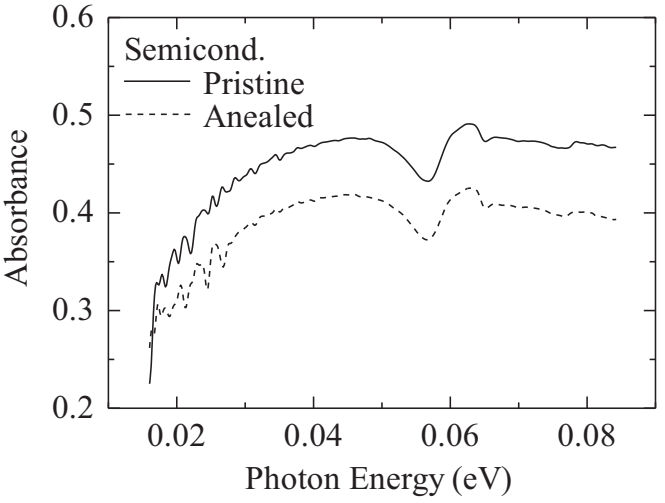

Fig. 5. IR absorption spectra for pristine (solid curve) and annealed (dashed curve) semiconducting SWNTs. Dip structures around 0.057 eV are instrumental origins.

properties of SWNTs are strongly affected by the chemical environment [18–21], and exposure to air or oxygen makes the SWNTs electrical resistance decreases dramatically [18]. This means that the SWNTs are doped by the adsorbed gas molecules, and semiconducting SWNTs are partially converted to metallic. Such doped electrons in semiconducting SWNTs also show plasmon resonance. By annealing the sample, adsorbed gas molecules on semiconducting SWNTs desorb, which makes the IR band due to plasmon resonance reduce.

4. Conclusion

In summary, the effect of e-beam irradiation on absorption and Raman spectra have been measured. By the irradiation of e-beam on SWNTs thin films, the intensity of Raman D-mode increases which is connected to defects increase, and the peak energy of IR absorption bands shift to the higher energy side. The peak energy is proportional to the inverse of G/D ratio. These results indicate that the origin of infrared band is due to the plasmon resonance of finite-length SWNT which is determined by the defect density.

Acknowledgments

We would like to thank to Prof. T. Aoki-M. and Dr. Morimoto for valuable discussions. This work was performed at SPring-8 with the approval of the Japan Synchrotron Radiation Research Institute, Proposal No.2012B1341, 2013A1258, 2014B1173, and 2015B1549. This work was partially supported by KAKENHI (25400331) and a matching fund subsidy for private universities from the Ministry of Education, Culture, Sports, Science and Technology, Japan.

References

[1] M. Ichida, S. Saito, Y. Kiyohara, T. Nakano, Y. Miyata, H. Kataura, H. Ando, J. Appl. Phys. 109 (2011) 113508.
[2] T. Ando, J. Phys. Soc. Jpn. 66 (1997) 1066.
[3] H. Kataura, Y. Kumazawa, Y. Maniwa, I. Umezu, S. Suzuki, Y. Ohtsuka, Y. Achiba, Synth. Met. 103 (1999) 2555.
[4] M. Ichida, S. Mizuno, Y. Tani, Y. Saito, A. Nakamura, J. Phys. Soc. Jpn. 68 (1999) 3131.
[5] M. Ichida, S. Mizuno, Y. Saito, H. Kataura, Y. Achiba, A. Nakamura, Phys. Rev. B 65 (2002) 241407.
[6] A. Ugawa, A.G. Rinzler, D.B. Tanner, Phys. Rev. B. 60 (1999) R11305.
[7] N. Akima, Y. Iwasa, S. Brown, A.M. Barbour, J.B. Cao, J.L. Musfeldt, H. Matsui, N. Toyota, M. Shiraishi, H. Shimoda, O. Zhou, Adv. Mater. 18 (2006) 1166.
[8] T. Kampfrath, K. von Volkmann, C.M. Aguirre, P. Desjardins, R. Martel, M. Krenz, C. Frischkorn, M. Wolf, L. Perfetti, Phys. Rev. Lett. 101 (2008) 267403.
[9] M. Ichida, S. Saito, T. Nakano, Y. Feng, Y. Miyata, K. Yanagi, H. Kataura, H. Ando, Solid State Commun. 151 (2011) 1696.
[10] T. Morimoto, S.-K. Joung, T. Saito, D.N. Futaba, K. Hata, T. Okazaki, ACS Nano 8 (2014) 9897.
[11] N. Hamada, S. Sawada, A. Oshiyama, Phys. Rev. Lett. 68 (1992) 1579.
[12] C.L. Kane, E.J. Mele, Phys. Rev. Lett. 78 (1997) 1932.
[13] Y. Akai, S. Saito, Physica E 29 (2005) 555.
[14] Y.K. Kwon, S. Saito, D. Tomanek, Phys. Rev. B. 58 (1998) R13314.
[15] M.S. Arnold, A.A. Green, J.F. Hulvat, S.I. Stupp, M.C. Hersam, Nat. Nanotechnol. 1 (2006) 60.
[16] T. Nakanishi, T. Ando, J. Phys. Soc. Jpn. 78 (2009) 114708.
[17] Y. Miyata, K. Shiozawa, Y. Asada, Y. Ohno, R. Kitaura, T. Mizutani, H. Shinohara, Nano Res. 4 (2011) 963.
[18] P.G. Collins, K. Bradley, M. Ishigami, A. Zettl, Science 287 (2000) 1801.
[19] G.U. Sumanasekera, C.K.W. Adu, S. Fang, P.C. Eklund, Phys. Rev. Lett. 85 (2000) 1096.
[20] S.-H. Jhi, S.G. Louie, M.L. Cohen, Phys. Rev. Lett. 85 (2000) 1710.
[21] H.E. Romero, G.U. Sumanasekera, S. Kishore, P.C. Eklund, J. Phys.: Cond. Matt 16 (2004) 1939.